THE ASTROPHYSICAL JOURNAL, 564:792–802, 2002 January 10

INTERSTELLAR AND CIRCUMSTELLAR REACTION KINETICS OF Na^+, Mg^+, AND Al^+ WITH CYANOPOLYYNES AND POLYYNES

ROBERT C. DUNBAR
Chemistry Department, Case Western Reserve University, Cleveland, OH 44106; rcd@po.cwru.edu

AND

SIMON PETRIE
School of Chemistry, University College, University of New South Wales, Australian Defence Force Academy, Canberra, ACT 2600, Australia; and Department of Chemistry, Australian National University, Canberra, ACT 0200, Australia; spetrie@rsc.anu.edu.au
Received 2001 April 5; accepted 2001 September 5

ABSTRACT

We report calculated rate coefficients for the radiative association reactions of M^+ (Na^+, Mg^+, or Al^+) with cyanopolyynes $HC_{2n+1}N$ ($n = 0$–4) and polyynes $HC_{2n}H$ ($n = 1$–5), at temperatures relevant to conditions within dense interstellar clouds and the outer envelopes of mass-losing stars. These reaction rate coefficients were determined via variational transition state theory kinetic modeling calculations employing structural, energetic, and spectroscopic parameters obtained from density functional theory calculations. We have performed simple kinetic modeling of these reactions within a cold dark cloud (TMC-1) and within the outer envelope of a C-rich, post–asymptotic giant branch mass-losing star (IRC +10216), with molecular compositions and other parameters of these environments taken from current chemical models. This modeling indicates that the highly efficient radiative association reactions of Mg^+ and Al^+ with HC_5N and HC_7N, and of Na^+ with HC_7N, give a drastic reduction in the lifetime of the atomic metal ions in these environments compared with a model in which radiative recombination of M^+ with e^- is the sole metal-ion loss process. These results also provide further support to the hypothesis that M^+/cyanopolyyne reactions are the route to metal cyanide radicals such as MgCN and MgNC in cold astrophysical environments.

Subject headings: circumstellar matter — ISM: clouds — ISM: molecules — molecular processes — stars: individual (IRC +10216) — stars: winds, outflows

1. INTRODUCTION

Metal ions M^+ (M = Na, Mg, Fe, ...) are considered to be major carriers of positive charge within dense interstellar clouds and circumstellar envelopes (Graedel, Langer, & Frerking 1982; de Boisanger, Helmich, & van Dishoeck 1996; Caselli et al. 1998). Traditionally, the sole or dominant loss process considered for these ions within models of interstellar chemistry (Oppenheimer & Dalgarno 1974; Millar et al. 1991; Lee, Bettens, & Herbst 1996) has been that of radiative recombination with electrons,

$$M^+ + e^- \rightarrow M + h\nu\ , \qquad (1)$$

a reaction of generally low efficiency. The notion that radiative association reactions of metal ions

$$M^+ + X \rightarrow MX^+ + h\nu \qquad (2)$$

could provide an alternative loss process for these ions was first raised almost two decades ago (Millar 1982) but has since received little attention, owing to the absence of reliable experimental or theoretical data on the efficiency of reaction (2). Nevertheless, reactions of this type are potentially important for several reasons: they permit metal-containing ion neutralization by the much more efficient process of dissociative recombination, e.g.,

$$MX^+ + e^- \rightarrow M + X\ ; \qquad (3)$$

they mitigate the discrepancies with observed molecular abundances typically associated with "high-metal models" of interstellar or circumstellar chemistry (see, for example, Caselli et al. 1998); and they provide possible pathways (Petrie 1996) to metal-containing neutrals detectable by radioastronomy, thereby yielding data on the metallic components within cold astrophysical environments.

The circumstellar metal-containing molecules detected to date—most of them around the carbon-rich, post–asymptotic giant branch (AGB) star IRC +10216—fall into two categories: even-electron species such as AlF, KCl, and Na(CN) (Cernicharo & Guélin 1987; Turner, Steimle, & Meerts 1994; Ziurys, Apponi, & Phillips 1994) are found in the warm inner envelope (Guélin, Lucas, & Nevi 1997), while the magnesium-containing radicals MgCN and MgNC (Kawaguchi et al. 1993; Ziurys et al. 1994; Guélin et al. 1995) attain peak abundance in the cold outer envelope (Guélin, Lucas, & Cernicharo 1993). It has been proposed (Petrie 1996) that the latter radicals are formed by reaction sequences initiated by processes of type (2) involving Mg^+ and the cyanopolyynes $HC_{2n+1}N$, which are known to be highly abundant in IRC +10216.

Other recent developments in circumstellar chemistry also affect our understanding of metal chemistry in such environments. Detection of MgNC within two other astrophysical sites, the proto–planetary nebulae AFGL 618 and AFGL 2688 (Highberger, Savage, & Ziurys 2000) now means that IRC +10216 need no longer be regarded as a unique astrophysical environment: an understanding of its circumstellar chemistry will be valuable for other objects also. Moreover, the recent observation (Ziurys et al. 2001) of AlNC in IRC +10216 gives further interest to the aluminum chemistry in such objects. Finally, the observation of HC_4H and HC_6H around AFGL 618 (Cernicharo et al. 2001) has now proved the existence of a long-suspected class of large interstellar and circumstellar molecules, the

polyynes. These are excellent prospective reactants in radiative association reactions such as reaction (2).

While the difficulties associated with laboratory measurement of radiative association rate coefficients, particularly at low temperatures, remain severe, the computational treatment of radiative association (RA) kinetics has become quite sophisticated. Using approaches such as variational transition state theory, with input data obtained from quantum chemical calculations, it has become possible to determine RA rate coefficients to a useful level of accuracy. The necessary computed parameters are IR vibrational frequencies and intensities, binding energies, and ion and neutral structures. In earlier work (Petrie & Dunbar 2000), we investigated the prospects for reaction (2) between Na^+, Mg^+, or Al^+ and a set of small- to medium-sized interstellar molecules such as H_2, CO, c-C_3H_2, and HC_3N. Our conclusion was that such reactions were unable to outweigh the occurrence of radiative recombination (1) as loss processes for the metal ions considered, but that association with larger neutrals might compete with process (1). In the present work, we examine this possibility further, by studying the RA kinetics of Na^+, Mg^+, and Al^+ with the cyanopolyynes $HC_{2n+1}N$ ($n = 0$–4) and with the polyynes $HC_{2n}H$ ($n = 1$–5). The goal of the present work is to assess the importance of these RA reaction pathways on the metal-ion chemistry included in the current chemical models of cold astrophysical environments, in which these channels have up to now not been included in a realistic way. Thus our calculated rate constants are combined with the molecular abundances and physical parameters of existing chemical models to give new estimates of metal-ion lifetimes and new perspectives on the polyyne and cyanopolyyne chemistry.

2. THEORETICAL METHODS

2.1. *Calculation of Energetic and Spectroscopic Parameters*

All quantum chemical calculations described here employed the density functional procedure with the B3-LYP functional, using the GAUSSIAN 98 quantum chemistry program suite (Frisch et al. 1998). Density functional theory has been widely shown to yield accurate results for molecular structures (see, for example, Kieninger et al. 1998) and vibrational frequencies (Scott & Radom 1996), and good agreement with experimentally determined bond energies (Curtiss et al. 1997), at modest computational expense. Geometry optimizations and frequency calculations were performed using the "correlation-consistent" cc-PVDZ basis sets of Dunning (1989) for H, C, and N atoms and the following basis sets for the metal atoms: for Na and Mg, the augmented double-zeta ANO basis sets of Roos and coworkers (Widmark, Persson, & Roos 1991), and for Al, the augmented correlation-consistent aug-cc-PVDZ basis set (Woon & Dunning 1993). We denote these basis set combinations as aug-DZ for brevity in the discussion that follows. All vibrational frequencies, IR intensities, moments of inertia, and zero-point energies obtained from the B3-LYP/aug-DZ calculations were used without subsequent correction or scaling.

For several species, particularly the metal-ion adducts of the smaller neutrals, additional calculations were made using larger basis sets, which we denote as TZ and as aug-TZ. The TZ basis set, used only for sodium-containing ions, features cc-PVTZ basis sets (Dunning 1989) for H, C, and N and a truncated version of Soldán, Lee, & Wright's (1998) AVTZ basis set for Na. This truncated sodium basis set, constructed by removing the outermost *sp*, *d*, and *f* functions from the AVTZ basis, has undergone extensive testing (Petrie 2001) and performs well for the purposes of geometry optimization and determination of single-point energies. The aug-TZ basis set combination also employs cc-PVTZ bases for H, C, and N, in conjunction with the AVTZ sodium basis set (Soldán, Lee, & Wright 1998), the augmented triple-zeta ANO basis set for magnesium (Widmark et al. 1991), or the augmented correlation-consistent aug-cc-PVTZ basis set for aluminium (Woon & Dunning 1993). In most cases, these larger basis set combinations were used only for single-point total energy determinations; however, for some of the metal ion/polyyne adducts, geometry optimization using a larger basis set than aug-DZ was desirable so as to identify the relative energies of different isomeric adducts properly.

The performance of B3-LYP and other density functional methods for calculating dipole moments and polarizabilities (and, one expects, for quadrupole moments also) has been reported to be comparatively poor for extended conjugated-pi systems (of which the larger cyanopolyynes and polyynes are examples). As shown in Table 1, our calculated parameters for HCCH and HCN are more or less close to established literature values, but we were not able to make such comparisons for the larger systems. Champagne et al. (2000) have reported that, while these methods typically perform well for dipole moments and polarizabilities for smaller molecules, they appear to overestimate these values systematically by an increasingly large factor for large conjugated species (e.g., by a factor of 2 for 20-C conjugated chains). Notwithstanding this deficiency in the B3-LYP methodology, we have used this method for calculation of multipole moments and polarizabilities in the

TABLE 1

PROPERTIES OF $HC_{2n}H$ AND $HC_{2n+1}N$

X	μ[a]	Q[b]	α[c]		
			$\perp$	$\parallel$	Mean
HCCH ...	0	6.4 (6.4[d])	1.41	4.35	2.39 (3.4[e])
HC_4H	0	12.5	2.43	12.4	5.75
HC_6H	0	19.8	3.38	25.8	10.9
HC_8H	0	28.1	4.44	45.2	18.0
$HC_{10}H$ ...	0	37.4	5.53	71.1	27.4
HCN	2.80 (3.00[f])	1.9 (2.2[g])	1.27	2.97	1.84 (2.5[h])
HC_3N	3.65	2.2	2.26	9.64	4.72
HC_5N	4.40	1.7	3.34	21.4	9.36
HC_7N	5.09	0.8	4.48	39.0	16.0
HC_9N	5.71	0.7	5.51	63.2	24.7

NOTE.—Calculated parameters for the neutrals $HC2_nH$ and $HC2_{n+1}N$ obtained at the B3-LYP/cc-PVDZ level of theory, along with some consensus literature values.

[a] Dipole moment, in debyes.

[b] Quadrupole moment, in debyes-angstroms (center of mass origin). The moment Q (Buckingham definition; Buckingham 1967) is calculated from the computed Cartesian components Θ_{ii} (Hirschfelder et al. 1964), using $Q = \Theta_{zz} - \Theta_{xx}$.

[c] Polarizability, in Å^3.

[d] Russell & Spackman 1996; Halkier & Coriani 1999; Watson 1995; Coonan & Ritchie 1993.

[e] Russell & Spackman 1996; Kumar & Meath 1992.

[f] Maroulis & Pouchan 1998; Bhattacharya & Gordy 1960.

[g] Maroulis & Pouchan 1998.

[h] Maroulis & Pouchan 1998; Spackman 1989.

present work for reasons of computational feasibility and consistency (since all other parameters used here were obtained from B3-LYP). Our largest systems may thus incur some error in collision rates on this account, but such errors are not expected to be important compared with other uncertainties.

2.2. *Variational Transition State Theory Calculations*

Variational transition state theory (VTST) provides a reliable and convenient way to calculate the radiative association rate constants needed (Klippenstein et al. 1996; Truhlar, Garrett, & Klippenstein 1996). The assumptions of the VTST approach to kinetics are expected to be valid to excellent accuracy for the large-distance transition states involved in these reactions. Quantum chemical calculations of the molecular quantities needed as inputs for the VTST calculation are subject to various uncertainties, but can be used with confidence at the levels of accuracy needed for astrophysical applications as described here. The use of the VariFlex kinetics package[1] to implement the VTST approach was described in our previous publication (Petrie & Dunbar 2000), and similar methods were used here. The calculation is carried out for ranges of the conserved quantities E (total energy) and J (total angular momentum), and the resulting rate constants are convoluted over a thermal distribution of reactants.

The model calculations described below indicate that the kinetic effects of short-range repulsions and polarizability anisotropies in these systems are negligible. Accordingly, only long-range potentials were used, specifically the ion–induced-dipole (spherically averaged), ion-dipole, and ion-quadrupole interactions. Polarizabilities, dipole moments, and quadrupole moments were taken from the quantum calculations, as shown in Table 1.

For ion-neutral systems dominated by long-range interactions, the dynamical aspects of the collision and redissociation processes are fairly easy to calculate with confidence, and the ultimate accuracy of the RA kinetics predictions in calculations like the present ones is probably limited by uncertainties in the binding energy and the infrared radiative properties of the complex. There is limited experience in assessing the absolute accuracy of such RA rate coefficient predictions for polyatomic systems, but our experience (Dunbar 1994; Ryzhov, Klippenstein & Dunbar 1996; Ryzhov & Dunbar 1997; Ryzhov et al. 1998; Gapeev et al. 2000) gives the hope that the predicted absolute values are useful within a factor of 2 or 3 and are not likely to err by as much as an order of magnitude.

3. RESULTS AND DISCUSSION

3.1. *Structural and Energetic Trends*

Key structural parameters used in this work, for ion adducts and the corresponding neutral molecules, are given in Tables 1–3. Calculated metal-ligand bond energies are given in Table 4.

We anticipate that binding energies determined using the larger aug-TZ basis sets are more accurate than the aug-DZ values. Calculations using the aug-TZ bases were feasible only for the small- to medium-sized adducts: comparison of the aug-DZ and aug-TZ metal-ligand bond energies for these species showed that the aug-DZ values exceeded the corresponding aug-TZ values, typically by around 6 kJ mol^{-1}. The aug-TZ values generally showed acceptable agreement with existing high-level ab initio values, such as those obtained using G2 theory (Petrie & Dunbar 2000). In consequence, we have lowered the aug-DZ bond energies listed in Table 4 by 6 kJ mol^{-1}, when calculating rate coefficients for the reactions of M^+ with cyano-

TABLE 2

$MHC_{2n}H^+$ Rotational Parameters

MX^+	σ[a]	A[b]	B[b]	C[b]
$Na(HC_2H)^+$[c]	2	35.5	6.12	5.22
$Na(HC_4H)^+$ (1)[c]	2	5.18	4.42	2.39
$Na(HC_6H)^+$ (1, TS)[c,d]	2	4.42	1.33	1.02
$Na(HC_6H)^+$ (2)[c]	1	5.45	1.14	0.943
$Na(HC_8H)^+$ (1)	2	4.40	0.560	0.496
$Na(HC_8H)^+$ (2)	1	5.25	0.466	0.428
$Na(HC_{10}H)^+$ (1, TS)[d]	2	4.07	0.289	0.270
$Na(HC_{10}H)^+$ (2)	1	4.39	0.283	0.266
$Na(HC_{10}H)^+$ (3)	1	5.17	0.239	0.229
$Mg(HC_2H)^+$	2	34.5	6.23	5.28
$Mg(HC_4H)^+$ (1)	2	5.38	4.34	2.40
$Mg(HC_4H)^+$ (2)	1	12.9	1.94	1.69
$Mg(HC_6H)^+$(1, TS)[d]	2	4.52	1.31	1.01
$Mg(HC_6H)^+$ (2)	1	10.6	0.716	0.671
$Mg(HC_8H)^+$ (1)	2	4.70	0.559	0.500
$Mg(HC_8H)^+$ (2)	1	9.32	0.344	0.331
$Mg(HC_{10}H)^+$ (1, TS)[d]	2	4.20	0.289	0.271
$Mg(HC_{10}H)^+$ (2)	1	4.68	0.283	0.267
$Mg(HC_{10}H)^+$ (3)	1	8.61	0.191	0.187
$Al(HC_2H)^+$[e]	2	35.4	5.06	4.42
$Al(HC_4H)^+$ (1)[e]	2	4.37	4.35	2.18
$Al(HC_4H)^+$ (2)[e]	1	10.8	1.96	1.66
$Al(HC_6H)^+$ (1, TS)[d,e]	2	3.86	1.33	0.990
$Al(HC_6H)^+$ (2)[e]	1	4.84	1.13	0.914
$Al(HC_6H)^+$ (3)[e]	1	9.39	0.712	0.662
$Al(HC_8H)^+$ (1)	2	3.91	0.560	0.489
$Al(HC_8H)^+$ (2)	1	8.47	0.332	0.320

Note.—Calculated rotational parameters for the molecular ions $MHC_{2n}H^+$, obtained at B3-LYP/aug-DZ or at a higher level of theory. Unless otherwise specified, the aug-DZ basis was used for all atoms in the indicated structure.

[a] Rotational symmetry number of the ion MX^+.

[b] Rotational constant of MX^+, in GHz.

[c] Basis set employed: TZ (see text).

[d] TS designates structures exhibiting one imaginary vibrational frequency.

[e] Basis set employed: aug-TZ.

TABLE 3

$HC_{2n+1}N^+$ Rotational Parameters

	$B_e(MX^+)$[a]		
X	M = Na	M = Mg	M = Al
HCN	4.34	4.66	4.03
HC_3N	1.33	1.38	1.26
HC_5N	0.568	0.579	0.544
HC_7N	0.293	0.296	0.282
HC_9N	0.170	0.172	0.164

Note.—Calculated rotational parameters for the molecular ions $HC_{2n+1}N^+$, obtained at the B3-LYP/aug-DZ level of theory. The basis set combinations are defined in the text.

[a] Rotational constant of MX^+, in GHz.

[1] S. J. Klippenstein, A. F. Wagner, R. C. Dunbar, D. M. Wardlaw, S. H. Robertson, & E. W. Diau 1998, VariFlex computer code, available at http://chemistry.anl.gov/chem-dyn/VariFlex/.

TABLE 4

BINDING ENERGIES

X	$D(M^+-X)$ M = Na	M = Mg	M = Al
HCCH.....	59.9 (a3)	76.3 (a3)	60.4 (a3)
HC_4H (1)[a].....	67.3 (a3)	81.2 (TS) (a3)	73.6 (a3)
HC_4H (2).....	...	88.1 (a3)	73.3 (a3)
HC_6H (1)[a].....	68.5 (TS) (a3)	84.5 (TS) (a2)	78.2 (TS) (a3)
HC_6H (2).....	71.3 (a3)	101.5 (a2)	82.2 (a3)
HC_6H (3).....	...	...	89.4 (a3)
HC_8H (1).....	78.2 (a2)	103.3 (a2)	76.4 (a3)
HC_8H (2).....	81.3 (a2)	129.2 (a2)	96.2 (a3)
$HC_{10}H$ (1)[a].....	80.2 (TS) (a2)	110.1 (TS) (a2)	
$HC_{10}H$ (2)	81.8 (a2)	110.8 (a2)	
$HC_{10}H$ (3)	84.9 (a2)	138.1 (a2)	
HCN.....	110.6 (a3)	135.8 (a3)	110.3 (a3)
HC_3N	124.1 (a3)	157.9 (a3)	135.6 (a3)
HC_5N	134.3 (a3)	184.5 (a2)	155.5 (a3)
HC_7N	148.8 (a2)	197.4 (a2)	175.4 (a2)
HC_9N	154.3 (a2)	206.8 (a2)	186.4 (a2)

NOTE.—Calculated metal/ligand binding energies (kJ mol^{-1}) for the molecular ions $MHC_{2n}H^+$ and $MHC_{2n+1}N^+$ obtained at the indicated level of theory. These values include ZPE and are not corrected for BSSE. a3 = aug-TZ basis set; a2 = aug-DZ basis. It is recommended that the aug-DZ values shown here should be adjusted downward by 6 kJ mol^{-1}.

[a] TS designates structures exhibiting one imaginary vibrational frequency.

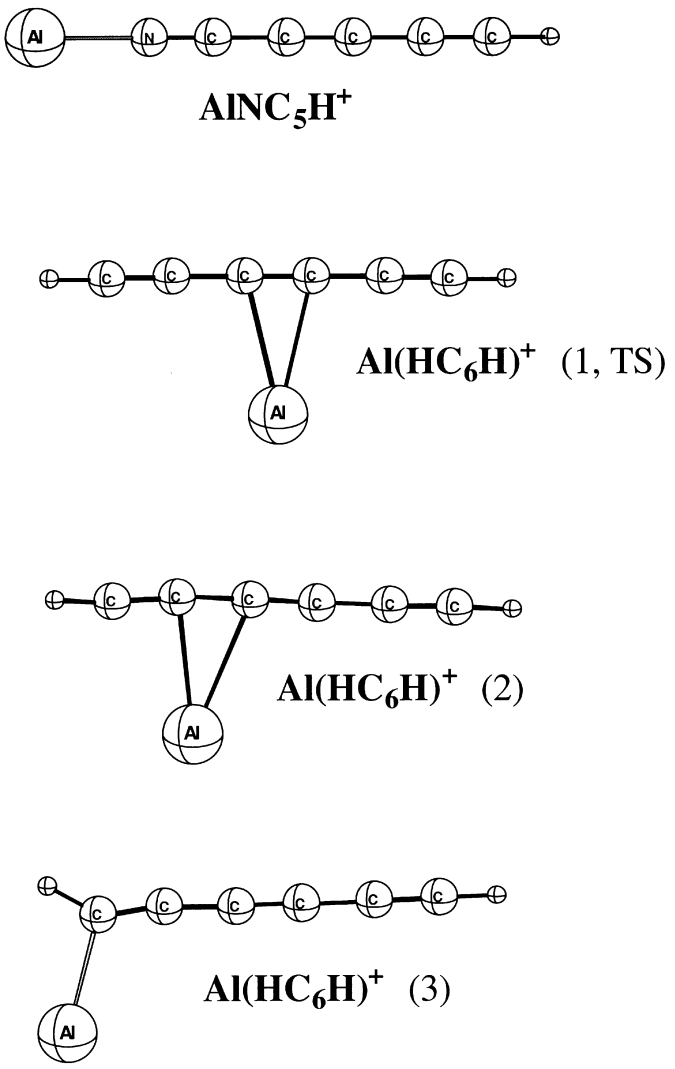

FIG. 1.—B3LYP/cc-PVTZ optimized geometries for stationary points obtained on the $Al(NC_5H)^+$ and $Al(HC_6H)^+$ potential energy surfaces.

polyynes, and for Na^+ and Al^+ with polyynes. For the Mg^+/polyyne species, a somewhat larger discrepancy was evident between aug-DZ and aug-TZ values, and for these species we recommend devaluation of the aug-DZ bond strengths by 9 kJ mol^{-1}.

The calculated binding energies for metal ion/cyanopolyyne adducts increase from Na^+ to Al^+ to Mg^+ and also increase in traversing the sequence of cyanopolyynes from HCN to HC_9N. The trend in bond energies for the different metal ions is consistent with that seen for other ligands, as shown for example in our earlier study on M^+ with small interstellar molecules (Petrie & Dunbar 2000). The regularity in bond energies is matched by the structural uniformity of these adducts—in all cases, the adduct ion is a linear species stabilized by σ-donation from the terminal N of the cyanopolyyne to the metal atom.

Greater diversity is seen for the polyyne complexes. Our initial optimizations on these adducts were on C_{2v} structures featuring M^+ coordination with the polyyne's center of mass: it soon became evident that such structures were not always true minima on their respective potential energy surfaces. We have located local minima that correspond to M^+ coordination with virtually any of the C—C single bonds within a given polyyne; for Al^+, structures were also found that involved coordination with a C—H bond. In general, metal/ligand bond strengths were highest for the coordination of the metal atom at the site farthest from the polyyne's center of mass. In the sections that follow, we have identified isomeric M^+/polyyne structures as (1), (2), (3) etc.: the larger the numeric value, the greater the displacement of the M^+ coordination site from the polyyne's centre of mass. In all cases, structure (1) designates coordination at the central C—C bond. Representative structures, for Al^+ with HC_5N and HC_6H, are shown in Figure 1.

3.2. *Model Calculations on a Hypothetical Linear Molecule*

Many of the known interstellar molecules, including both classes of neutrals considered in the present study, have long, thin shapes. Neutral partners with this shape take on extreme values of various properties affecting the kinetics of the metal-ion reactions. Among these are (i) dipole moment, (ii) quadrupole moment, (iii) polarizability anisotropy, and (iv) repulsive interaction radius. Before considering kinetics of reactions with specific ions and neutrals, it will be useful to survey the possible importance of such effects using a model system.

Accurate estimation of the kinetic effects of these interactions is easy only for the ion-dipole term, for which a convenient approximate expression has been derived from trajectory modeling (Su & Chesnavich 1982). VTST provides a convenient framework for adding the other interactions to the basic isotropic ion–induced-dipole interaction that normally dominates low-temperature ion-neutral collisions. The maximum possible effect on the radiative association kinetics of adding a particular potential energy term can be assessed by a VTST calculation of the change in the ion-neutral capture rate.

The model neutral molecule has the approximate shape and properties of HC_9N. This typifies the cyanopolyyne family, which have large dipole moments, strongly anisotropic polarizabilities, and short-range repulsive contacts onsetting at large center-of-mass separations. Furthermore, by setting the dipole moment to zero and adding a quadrupole moment, this same model can be adapted to represent the polyyne family, characterized by large quadrupole moments, strongly anisotropic polarizabilities, and repulsive contacts. The model has the following parameters:

isotropic polarizability: 23.5 Å^3

parallel polarizability: 62.0 Å^3

perpendicular polarizability: 4.4 Å^3

dipole moment: 6.0 debye

quadrupole moment: 37.0 debye-Å

atomic diameters (Å): 1.4(C), 1.7(N), 1.1(H), 6.0(M^+) .

[This quadrupole moment, which was used for the polyyne model calculation, is defined as $Q_2^0 = (\Theta_{zz} - \Theta_{xx})$ as in Hirschfelder, Curtiss, & Bird 1964.] The calculated capture rates for various combinations of potential terms are shown in Table 5. We summarize the effects in Table 5.

3.2.1. *Anisotropic Polarizability*

The comparison of the capture rates using the anisotropic polarizability (A) versus the average isotropic polarizability (P) shows an increase of the order of 10% at the lowest temperatures, and even less at high temperatures. Rotational averaging of the polarizability is nearly complete at the intermolecular separation corresponding to the transition state. Thus the anisotropy of the charge-polarizability interaction gives at most a minor perturbation to the collision rate. In further calculations (not shown in Table 5) that combined the polarizability with other potential terms, the effect of polarizability anisotropy was likewise found to be small, affecting rates by less than 10%.

3.2.2. *Long-Range Potentials*

Dipole moment.—As expected, the large dipole (P + D) in this system gives a major increase in capture rate relative to the no-dipole rate (P), approaching an order-of-magnitude increase at the lowest temperatures and a factor of 2.5 at room temperature.

Quadrupole moment.—The quadrupole interaction has shorter range (r^{-3}) than the dipole interaction (r^{-2}), which makes it considerably less important. It is seen that the increase in capture rate upon adding a quadrupole interaction (P + Q), relative to the polarizability-only value (P), is of the order of a factor of 2 at low temperatures and somewhat less at high temperatures.

TABLE 5

COLLISION RATES FOR MODEL SYSTEM

Interactions	50 K	300 K
P.....	31.4 ± 0.5	29.0 ± 0.5
A	34.0 ± 0.5	31.0 ± 0.5
D	171 ± 3	70 ± 1
Q	46 ± 1	31 ± 1
P+D.....	172 ± 3	79 ± 1
P+Q.....	55 ± 1	41 ± 1
A+H	34.2 ± 0.5	23.7 ± 0.5

NOTE.—Collisional rate constants (10^{-10} cm^3 molecule^{-1} s^{-1}) calculated by VTST for the model molecule colliding with Na^+. P = average isotropic polarizability; A = anisotropic polarizability; D = dipole; Q = quadrupole; H = hard-sphere repulsions. Quoted uncertainties reflect only the statistical uncertainty arising from Monte Carlo integration and are not realistic estimates of the actual accuracy of the VTST approach.

3.2.3. *Short-Range Repulsions*

At 300 K the transition state for a typical E and J is at a distance of ~9 Å, which is similar to the hard-sphere contact distance in the most interacting orientation with a large metal ion, so there is at least the possibility that hard-sphere repulsions might affect the capture rate. At low temperatures where the typical transition state is at a distance greater than 15 Å, there is no likelihood of a hard-sphere perturbation. The evaluation of hard-sphere repulsion effects by VTST is not entirely straightforward. The simple approach used here assumes that a collision gives non-capturing elastic scattering of the ion whenever the combination of energy and angular momentum allows the ion to make hard-sphere contact with the neutral in the most highly interacting orientation. This definitely gives an overestimate of the actual effect of short-range repulsive interactions on the ion-neutral capture rate. Table 5 shows that even with the extremely large metal-ion diameter used (6 Å), this estimated effect of hard-sphere repulsions on the capture rate is not large, reaching ~30% at room temperature.

3.2.4. *Summary*

From this model study, several conclusions apply to radiative association rate calculations for long molecules. Taking a threshold of a factor of 2 for a rate constant perturbation to have practical interest, the effect of the anisotropy of the polarizability, and likewise the effect of hard-sphere repulsions, can be ignored at all temperatures up to 300 K. If there is a dipole moment of the magnitude typical for cyanopolyynes, it is important at 300 K and very important at low temperatures. A quadrupole moment of magnitude typical of polyynes is borderline in importance over the entire temperature range. The long-range potential effects are not additive, but rather tend to be dominated by the longest range potential term.

These potential-function effects on the capture rates are relevant for association reactions occurring with near 100% collisional efficiency, but in the limit of low efficiency the strength and functional form of the ion-neutral potential become irrelevant to the radiative association rate. However, numerical tests show that the decline of the influence of intermolecular potentials on the kinetics is often quite slow with falling efficiency (Dunbar 1997). Even when the association efficiency is as low as one in 10^6, the presence of a large dipole moment, for instance, can markedly increase the calculated radiative association rate constant. So the kinetic simplification afforded by the limiting low-efficiency approximation can generally not be taken for granted without confirming calculations.

3.3. *Reaction Rates for* M^+

The calculated RA bimolecular reaction rate constants k_{ra} at various temperatures are displayed in Table 6 (polyynes) and Table 7 (cyanopolyynes). Also reported are

TABLE 6

RATE COEFFICIENTS FOR METAL-ION/POLYYNE SYSTEMS

T (K)	Na		Mg		Al	
	k_{ra}	k_{coll}	k_{ra}	k_{coll}	k_{ra}	k_{coll}
			MHC_4H^+			
10	6.99E−14	5.16E−09	6.13E−13	5.36E−09	1.67E−13	5.35E−09
30	1.49E−14	4.56E−09	1.37E−13	4.50E−09	3.56E−14	4.29E−09
100.....	2.57E−15	3.90E−09	2.37E−14	3.84E−09	6.09E−15	3.60E−09
300.....	2.50E−16	3.16E−09	2.31E−15	3.11E−09	5.90E−16	2.90E−09
			MHC_6H^+ (Structure 2)			
10	7.54E−12	4.83E−9	2.76E−10	3.82E−9	1.92E−10	3.80E−9
30	1.76E−12	4.33E−9	7.66E−11	3.70E−9	5.05E−11	3.36E−9
100.....	2.97E−13	3.48E−9	1.52E−11	3.33E−9	9.66E−12	3.02E−9
300.....	1.73E−14	2.66E−9	9.47E−13	2.66E−9	5.97E−13	2.70E−9
			MHC_8H^+ (Structure 2)			
10	5.6E−10	6.0E−9	5.6E−9	5.57E−9	4.48E−9	5.29E−9
30	1.5E−10	5.0E−9	4.7E−9	4.69E−9	2.76E−9	4.45E−9
100.....	2.0E−11	4.3E−9	2.9E−9	4.18E−9	9.05E−10	4.00E−9
300.....	4.0E−13	3.7E−9	2.4E−10	3.39E−9	3.10E−11	3.26E−9
			$MHC_{10}H^+$ (Structure 3)			
10	5.91E−9	6.98E−9	6.39E−9	6.39E−9		
30	3.43E−9	5.64E−9	5.54E−9	5.54E−9		
100.....	7.16E−10	5.06E−9	4.95E−9	4.98E−9		
300.....	7.58E−12	4.49E−9	1.99E−9	4.35E−9		

NOTE.—Radiative association rate constants and collision rate constants for metal-ion/polyyne systems (cm^3 $molecule^{-1}$ s^{-1}).

TABLE 7

RATE COEFFICIENTS FOR METAL-ION/CYANOPOLYYNE SYSTEMS

T (K)	Na		Mg		Al	
	k_{assoc}	k_{coll}	k_{assoc}	k_{coll}	k_{assoc}	k_{coll}
			MHC_3N^+			
10	8.30E−13	2.80E−8	2.00E−11	2.60E−8	1.30E−11	3.00E−8
30	1.80E−13	1.40E−8	4.30E−12	1.40E−8	2.70E−12	1.40E−8
100.....	2.80E−14	7.90E−9	6.80E−13	8.10E−9	4.50E−13	7.90E−9
300.....	2.90E−15	4.80E−9	7.00E−14	4.80E−9	4.60E−14	4.60E−9
			MHC_5N^+			
10	9.10E−10	2.00E−8	1.46E−8	1.85E−8	1.14E−8	1.75E−8
30	2.60E−10	1.40E−8	7.60E−9	1.23E−8	5.13E−9	1.17E−8
100.....	4.50E−11	9.50E−9	2.65E−9	9.33E−9	1.41E−9	8.79E−9
300.....	1.60E−12	5.70E−9	1.35E−10	5.65E−9	6.37E−11	5.55E−9
			MHC_7N^+			
10	3.76E−8	3.90E−8	4.16E−8	4.16E−8	3.26E−8	3.26E−8
30	1.65E−8	1.78E−8	1.94E−8	1.94E−8	1.58E−8	1.58E−8
100.....	5.93E−9	1.05E−8	1.07E−8	1.07E−8	9.86E−9	9.98E−9
300.....	2.15E−10	6.62E−9	3.41E−9	6.73E−9	2.74E−9	6.34E−9
			MHC_9N^+			
10	3.37E−8	3.37E−8	3.55E−8	3.55E−8	4.10E−8	4.10E−8
30	2.06E−8	2.06E−8	2.00E−8	2.00E−8	2.07E−8	2.07E−8
100.....	1.22E−8	1.24E−8	1.19E−8	1.19E−8	1.14E−8	1.14E−8
300.....	2.12E−9	7.59E−9	6.97E−9	7.40E−9	6.58E−9	6.98E−9

NOTE.—Radiative association rate constants and collision rate constants for metal-ion/cyanopolyyne systems (cm^3 $molecule^{-1}$ s^{-1}).

the rate constants k_{coll} for ion-neutral collision regardless of whether the complex is subsequently stabilized. It can be seen that in many cases the RA reactions approach unit collisional efficiency, in contrast to the situation with smaller neutral partners (Petrie & Dunbar 2000).

Some of the metal-ion/neutral pairs fall in the low-efficiency limit (the collisional efficiency of the reaction is low over the pertinent temperature range), while a number of other pairs fall in a high-efficiency limit (high collisional efficiency at all temperatures up to 300 K). In astrophysical environments, high cyanopolyyne or polyyne abundances are generally associated with $T < 50$ K, so a reaction in Table 6 or 7 can actually be considered as a high-efficiency case if it is highly efficient up to ~ 50 K. Reactions characterized as low efficiency will generally not be astrophysically important processes and would remain unimportant even if our calculated rate coefficients were revised upward by an order of magnitude, while those reactions which we calculate to be highly efficient are generally so close to saturation that a considerable reduction in metal-ligand bond strength, or in the rate of radiative emission, would be required to alter their tabulated rate coefficients. The reactions for which the actual magnitudes of the rate constants matter, and whose impact will be most difficult to assess reliably, are those which are of moderate, though not full, efficiency in this temperature range. These are notably Na^+ and Al^+ with HC_8H; Mg^+ with HC_6H; and Na^+, Mg^+, and Al^+ with HC_5N. For reactions of this last class, the astrophysical conclusions discussed below may be sensitive to uncertainty or inaccuracy in the quantum chemical data on which the VTST calculations are based.

4. IMPLICATIONS FOR INTERSTELLAR AND CIRCUMSTELLAR CHEMISTRY

Extensive efforts have been reported and are continuing in many laboratories to gather observational data on the properties and chemical compositions of cold, chemically rich interstellar environments and to fit these observations into global models of the chemistry. The end goal of the present work is to fit our calculated RA rate coefficients for the metal-ion reactions into the context of the current observational and modeling pictures. Reaction rates for this set of reactions are derived using environmental parameters and molecular densities of the neutral reactants taken from recent observations, where available, and from current chemical models. Reference to these current chemical models then provides the context for evaluating the significance of this class of reaction processes in the overall chemistry of cold clouds and circumstellar envelopes.

4.1. *Interstellar Clouds*

4.1.1. *Parameters for TMC-1 Modeling*

The interstellar cloud TMC-1 has been extensively observed, described and modeled. A temperature of 10 K was assumed here. Densities for HC_3N and for the polyynes were taken from the model of Millar, Farquhar, & Willacy (1997) and from experiment, as given by Langer et al. (1997). The other cyanopolyyne densities were scaled from HC_3N using the relative column densities reported by Bell et al. (1997).

4.1.2. *Chemical Implications for TMC-1*

The reactions of metal ions with the polyynes are too slow to have significance on the characteristic 10^6 yr evolution timescale of TMC-1. Table 8 shows the calculated lifetimes of the ions with respect to reactions with $HC_{2n}H$, none of which are shorter than 5×10^7 yr. On the other hand, as shown in Table 9, several of the cyanopolyyne reactions are important, perhaps even dominant, in the early cloud metal-ion chemistry. A number of them take much less than 10^6 yr.

These results show clearly the trade-off between increasing association rate constant and decreasing abundance as the size of the neutral partner grows. This is displayed graphically in Figure 2, which plots cyanopolyyne results from Table 9. With respect to length of the carbon chain, there is a very obvious optimal size around five to seven carbons at which this trade-off leads to the highest rates of reaction for these three metal ions in TMC-1.

The reactions of Mg^+ with HC_5N and of Na^+ with HC_7N in TMC-1 have the shortest timescales yet assigned to any Mg^+ or Na^+ loss processes involving known or postulated dense cloud constituents. Moreover, the M^+ lifetimes determined by the aggregate of these reactions, also shown in Table 9, are a few tens of thousands of years, which is small compared to the overall cloud lifetime. Although these lifetimes are 2 orders of magnitude longer than that of HCO^+ for instance, the most abundant poly-

TABLE 8

M^+/POLYYNE LIFETIMES IN TMC-1

		LIFETIME (yr)		
CARBON NUMBER	ABUNDANCE[a]	Na	Mg	Al
2	2.5E−08	4.1E+11	9.4E+10	2.2E+11
4	4.0E−11	1.2E+12	1.3E+11	4.9E+11
6	1.0E−10	4.4E+09	1.2E+08	1.7E+08
8	1.0E−11	5.9E+08	5.9E+07	7.2E+07
10	2.0E−12[b]	2.8E+08	2.5E+08	

NOTE.—Lifetime of M^+ against reaction with HC_nH in TMC-1 ($T = 10$ K, $[H_2] = 10^4$ cm^{-3}; from (Lee et al. 1996, new standard model; Millar et al. 1997).

[a] Fractional abundance of HC_nH relative to $[H_2]$ (Millar et al. 1997).

[b] Estimated by extrapolation.

TABLE 9

M^+/CYANOPOLYYNE LIFETIMES IN TMC-1

		M^+ LIFETIME (yr)		
CARBON NUMBER	ABUNDANCE[a]	Na^+	Mg^+	Al^+
3	6.0E−08	6.6E+07	2.8E+06	4.2E+06
5	4.0E−09	9.1E+05	5.7E+04	7.2E+04
7	1.0E−09	8.8E+04	7.9E+04	1.0E+05
9	5.0E−10	2.0E+05	1.9E+05	1.6E+05
e^-	5.0E−08	2.4E+06[b]	1.3E+06[b]	1.3E+06[b]
Aggregate[c]		5.5E+04	2.7E+04	3.2E+04

NOTE.—Lifetime of M^+ against reaction with HC_nN in TMC-1 ($T = 10$ K, $[H_2] = 10^4$ cm^{-3}; from Lee et al. 1996, new standard model; Millar et al. 1997).

[a] Molecule densities of HC_nN relative to $[H_2]$ from Ohishi & Kaifu 1998; e^- density (cm^{-3}; from Millar et al. 1997).

[b] Radiative recombination values α for the reaction of M^+ with e^- are 9.0×10^{-12} and 1.3×10^{-11} cm^3 s^{-1}, respectively, for Na^+ and Mg^+ (Millar et al. 1997); we have also used the Mg^+ value for Al^+.

[c] Lifetime corresponding to all reactions proceeding concurrently.

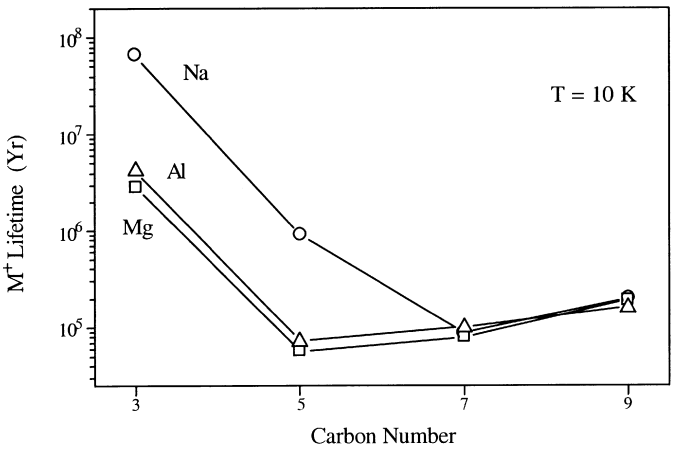

FIG. 2.—Lifetimes for the metal ions against reaction with cyanopolyyne molecules of varying carbon chain lengths in the cloud TMC-1.

atomic ion in most models (Millar et al. 1991), nevertheless it is clearly inappropriate to view these metal ions as inert and long-lived species. Since these radiative association processes occur 30 or 40 times faster than radiative recombination of the metal ions, it is also fallacious to assign radiative recombination as the only significant metal-ion loss process, as is done in existing models of cloud chemistry, and this is a shortcoming that must be addressed in future models. A further possible development from the inclusion of metal-ion radiative association reactions (see also Millar 1982; Petrie et al. 1997) may be the relaxation of stringent gas-phase metallic element depletions (Graedel et al. 1982) which are generally applied in models of dense cloud chemical evolution.

Metal-ion densities are not directly accessible to observation. Detailed chemical models (see, for example, Millar et al. 1991; Herbst & Leung 1986) estimate Na^+ and Mg^+ as ~25%–35% of the total positive charge content of a typical dense cloud, in the absence of radiative association as a metal-ion loss process. However, the present suggestion that the cyanopolyynes are reasonably effective scavengers of M^+ gives hope that future models will reassign a significant portion of the total metal content to experimentally observable polyatomic species, which would make it much easier to clarify the role of metals in the chemistry of cold astrophysical environments.

4.2. *Circumstellar Envelopes*

4.2.1. *Parameters for IRC +10216 Modeling*

Modeled temperatures vary depending on the model used and on the radial distance from the star; moreover, the kinetic temperature (needed for the rate modeling) is thought to differ somewhat from the excitation temperature usually measured by radioastronomy (Bell et al. 1992; Bieging & Tafalla 1993). Temperature assignments usually fall in the range 12–50 K. A kinetic temperature of 30 K will be adopted here for estimation purposes.

Column densities of $HC_{2n+1}N$ were taken from the survey of Kawaguchi et al. (1995). The molecule densities at the radius of the cyanopolyyne peak abundances are rather uncertain. Bieging & Tafalla (1993) estimated a peak HC_3N density (vs. $[H_2]$) of 7×10^{-7} at 4.7×10^{16} cm, and the other $HC_{2n+1}N$ peak densities can be scaled from this using the relative column densities of Kawaguchi et al. (1995). However, a shortcoming of this approach is that the Bieging & Tafalla data are from a BIMA millimeter interferometric study of rather limited (10″) angular resolution. Although the radius of the HC_3N shell according to these authors is consistent with that found by later studies, the thickness they found for this shell (15″) is much greater than that (~3″) found with the Plateau de Bure interferometer by Lucas, Guélin, and coworkers (see, for example, Lucas & Guelin 1998; Guélin et al. 1999); unfortunately, no direct abundance values have been assigned corresponding to these more recent Plateau de Bure observations. Since the cyanopolyynes are observed to be largely confined within a more compressed (and hence more concentrated) shell than was assumed in the analysis of the BIMA interferometer data, it seems appropriate to scale upward the density value derived from this study, along with the other $HC_{2n+1}N$ abundances that we anchor to it. Accordingly, we have multiplied the Bieging & Tafalla value of HC_3N density by a factor of 3, to obtain the peak abundance values listed in Table 10. This procedure is quite uncertain but will serve to illustrate the likely timescales of the M^+/cyanopolyyne reactions in the regions of high cyanopolyyne abundance.

4.2.2. *Chemical Implications*

The velocity of material outflow from IRC +10216 is $\sim 5 \times 10^{13}$ cm yr^{-1}, while its dimensions are of the order of 5×10^{17} cm, so reactions occurring faster than 10^4 yr can have significance for its chemical structure. Tables 10 and 11 assess the reaction rates of the metal ions with the cyanopolyynes in two ways. Using the estimated peak densities of the neutrals (at a radius of 5×10^{16} cm), the lifetimes of the ions are calculated on the assumption that they react with a steady supply of neutrals at this density (Table 10). It is seen that several of the reactions proceed on timescales considerably shorter than 10^4 yr.

Alternatively, the measured column densities can be used conveniently to estimate the integrated probability that a given metal ion will undergo association with a given neutral during its complete passage from the star out to

TABLE 10

M^+/CYANOPOLYYNE LIFETIMES IN IRC +10216

CARBON NUMBER	PEAK ABUNDANCE[a]	M^+ LIFETIME (yr)		
		Na^+	Mg^+	Al^+
3.....	2.1E−06	4.3E+06	1.8E+05	2.8E+05
5.....	3.3E−07	1.9E+04	650	970
7.....	1.8E−07	530	450	530
9.....	4.0E−08	2030	2100	2000
e^-	3.0E−08[b]	5.6E+06	3.8E+06	3.8E+06
Aggregate[c].....		510	260	350

NOTE.—Lifetime of M^+ against reaction with HC_nN in the region of maximum cyanopolyyne concentration (velocity = 1.45×10^6 cm s^{-1}: Bell et al. 1992; T = 30 K, $[H_2] = 2 \times 10^4$ cm^{-3}: Kwan & Linke 1982; Huggins 1995).

[a] Fractional abundance of HC_nN relative to $[H_2]$. Value for HC_3N from Bieging & Tafalla 1993 adjusted as described in the text; other values scaled from this using the relative values of Kawaguchi et al. 1995.

[b] From Doty & Leung 1998. Radiative recombination values used are as noted for Table 9.

[c] Lifetime corresponding to all reactions proceeding concurrently.

TABLE 11

M^+/Cyanopolyyne Depletions in IRC +10216

Carbon Number	Column Density[a]	M^+ Depletion (%)		
		Na^+	Mg^+	Al^+
3	1.5E+15	0	0	0
5	2.3E+14	2	45	33
7	1.3E+14	53	57	51
9	2.7E+13	18	17	18
e^-	9.2E+16[b]	25	34	34
Aggregate[c]		62	81	73

Note.—Depletion of M^+ due to reaction with HC_nN during transit of the ion through the reactive zone (velocity = 1.45×10^6 cm s^{-1}: Bell et al. 1992; $T = 30$ K).

[a] Molecule column density of HC_nN (cm^{-2}) from Kawaguchi et al. 1995. Note that these are total column densities, and not radial column densities as reported by Millar et al. 2000.

[b] Total e^- column density from radial column density calculated by Millar et al. 2000. Radiative recombination values used are as noted for Table 9.

[c] Depletion by reaction with all cyanopolyynes, but excluding e^- reactions.

large distances (Table 11). This probability is given by

$$P_{\text{association}} = 1 - \exp\left(-\frac{\rho k_{\text{ra}}}{2v}\right), \quad (4)$$

where ρ is the column density of the neutral, k_{ra} is the radiative association rate constant, v is the velocity of matter outflow from the star, and the factor of $\frac{1}{2}$ in the exponent arises because the ion traverses only half of the total column of neutrals. In Table 11 this probability is displayed as a percent depletion of the metal ion due to each given reaction, as well as the aggregate depletion expected when all of these reactions are occurring simultaneously. It is seen that the depletion of metal ions due to reaction with several of the individual cyanopolyynes is significant. Also shown in the table is depletion of the metal ion by radiative recombination with electrons, which is substantial. However, it should be noted that this refers to the total electron column density; the model of Doty & Leung (1998) suggests that most of this indicated depletion by electron recombination would occur at distances greater than the region of large cyanopolyyne abundance. The inefficiency of radiative recombination at the cyanopolyyne-peak radius is clear from Table 10. Looking at the aggregate depletions, it appears that a metal ion, particularly a Mg^+ or Al^+ ion, has a fairly poor chance of escaping from the stellar neighborhood without undergoing association with at least one cyanopolyyne neutral or recombination with an electron (or reaction by a pathway not considered here).

Just as with the interstellar cloud modeling, the circumstellar envelope results for cyanopolyynes in Table 10 and 11 indicate a clear range of carbon chain lengths, around five to seven carbons, for which the radiative association process has its greatest effect on metal-ion lifetimes. This is plotted for IRC +10216 in Figure 3.

It is difficult to verify a causal link between the M^+/cyanopolyyne radiative association reactions and circumstellar metal cyanide formation, because the crucial dissociative recombination reactions

$$MNC_{2n+1}H^+ + e \rightarrow \text{products} \quad (5)$$

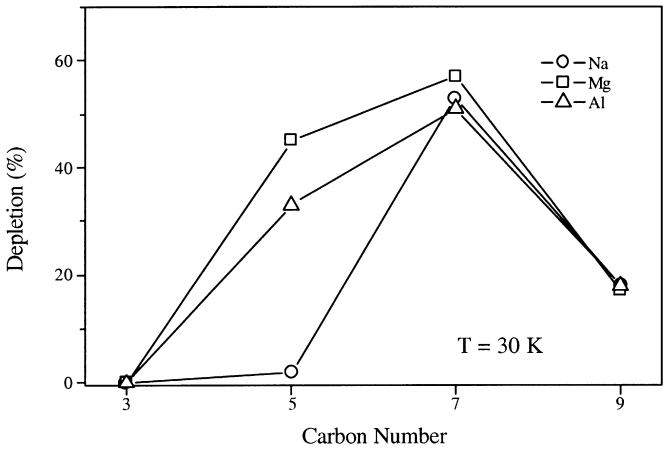

Fig. 3.—Depletion of metal ions by reaction with cyanopolyyne molecules of varying carbon chain lengths, as the ions pass through the circumstellar envelope IRC +10216 from the stellar neighborhood out to far distances.

have not been measured and the product distributions can only be conjectured (Petrie 1996, 1999). Nonetheless, the circumstantial evidence for reaction (5) as the route to M(NC) formation is strong. MgNC has to date been detected within three objects (IRC +10216, AFGL 618, and AFGL 2688) (Kawaguchi et al. 1993; Highberger et al. 2000), all of which have notably large column densities of HC_3N and HC_5N (Fukasaku et al. 1994) and detectable levels of cyanopolyynes as large as HC_9N (Bell et al. 1992; Truong-Bach, Graham, & Nguyen-Q-Rieu 1993, 1996); within IRC +10216, MgNC is found to occupy a thin spherical shell (Guélin et al. 1993) spatially coincident with the zone of peak abundances for the larger cyanopolyynes; and the very large rate coefficients that we find here for Mg^+ with HC_5N and larger cyanopolyynes, at temperatures appropriate to the outer envelope of IRC +10216, indicate that such radiative association reactions are efficient loss processes for the metal ion. Moreover, it is difficult to envisage other plausible low-temperature routes (i.e., having all steps exothermic and lacking activation barriers) to MgNC and MgCN: these metal cyanide radicals have a notably weak metal-ligand bond, in an environment where almost all species seen to date have chemical bonds at least 100 kJ mol^{-1} stronger.

The metal ion/cyanopolyyne mechanism may also very well account for the production of two further, recently detected CN-containing species, SiCN (Guélin et al. 2000) and AlNC (Ziurys et al. 2001). The possible formation of AlNC by such a pathway has already been proposed (Petrie 1996), while SiCN shares many features of MgCN and MgNC: it too is a radical with a comparatively weak metal-ligand bond (Largo-Cabrerizo 1988) and is apparently also confined to the cold outer envelope of IRC +10216 (Guélin et al. 2000), where a radiative association pathway would be most efficient.

The argument is made above for M^+/cyanopolyyne reactions as the dominant processes for metal-ion loss in IRC +10216. The effect of this chemistry on both M^+ abundances and also free electron abundances clearly needs further exploration; but there is an additional intriguing possibility. Do these M^+/cyanopolyyne reactions have a significant impact upon the abundances of the cyanopolyynes themselves? The observed MgNC column density

in IRC +10216 is in the range (2.5–5) $\times 10^{13}$ cm^{-2} (Guélin et al. 1995; Kawaguchi et al. 1995), which is only about 10% of the total $HC_5N+HC_7N+HC_9N$ column density (Kawaguchi et al. 1995), so it seems at first sight that extensive conversion of HC_nN into MgNC is not indicated. However, this fails to take into account the likelihood that MgNC has a shorter lifetime in IRC +10216 than the cyanopolyynes. Several properties of MgNC suggest that it might be readily destroyed by various reaction processes: it is a radical, possesses a weak bond between the ligand and an ionizable metal atom, and has a very large dipole moment. Thus the *reduction* in cyanopolyyne column density due to MgNC formation may substantially exceed the MgNC column density itself. This mode of cyanopolyyne removal has not been considered previously, but may be pertinent in light of the tendency of chemical models (see, for example, Millar & Herbst 1994; Millar, Herbst, & Bettens 2000) to overestimate significantly the abundance of HC_5N and the larger cyanopolyynes while recording reasonably good agreement for the HCN and HC_3N abundances.

5. CONCLUSIONS

Radiative association reactions between M^+ (Na^+, Mg^+, and Al^+) and cyanopolyynes as small as HC_5N or HC_7N approach collisional efficiency at temperatures of 10–30 K, appropriate to cold dark interstellar clouds and the outer regions of circumstellar envelopes such as IRC +10216. It appears that such reactions will generally dominate over M^+/electron radiative recombination reactions as a loss process for metal ions in cold astrophysical environments possessing substantial abundances of cyanopolyynes. This effect will necessitate significant modifications to existing kinetic models of dense cloud and circumstellar envelope chemical evolution.

Observations of metal cyanides such as MgNC, MgCN, and SiCN, species which appear capable of formation only via such radiative association reactions as we have examined here, may provide unprecedented opportunities for the determination of gas-phase metal abundances within cold dense astrophysical environments (and hence a measure of the partitioning of metals between the gas and dust phases) once the chemistry of these metal-containing molecules has been sufficiently worked out. Further work is needed to clarify the roles of metal-containing molecules in the chemical evolution of cold astrophysical environments.

S. P. thanks the School of Chemistry, University College, for the generous provision of computational resources. R. C. D. acknowledges the support of the donors of the Petroleum Research Fund, administered by the American Chemical Society. Text files containing the atomic coordinates, vibrational frequencies, and infrared intensities of all the adduct ions are available via email to spetrie@rsc.anu.edu.au.

REFERENCES

Bell, M. B., Avery, L. W., MacLeod, J. M., & Matthews, H. E. 1992, ApJ, 400, 551
Bell, M. B., Feldman, P. A., Travers, M. J., McCarthy, M. C., Gottlieb, C. A., & Thaddeus, P. 1997, ApJ, 483, L61
Bhattacharya, B. N., & Gordy, W. 1960, Phys. Rev., 119, 144
Bieging, J. H., & Tafalla, M. 1993, AJ, 105, 576
Buckingham, A. D. 1967, Adv. Chem. Phys., 12, 107
Caselli, P., Walmsley, C. M., Terzieva, R., & Herbst, E. 1998, ApJ, 499, 234
Cernicharo, J., Heras, A. M., Tielens, A. G. G. M., Pardo, J. R., Herpin, F., Guélin, M., & Waters, L. B. F. M. 2001, ApJ, 546, L123
Cernicharo, J., & Guélin, M. 1987, A&A, 183, L10
Champagne, B., Perpete, E. A., Jacquemin, D., vanGisbergen, S. J. A., Baerends, E.-J., Soubra-Ghaoui, C., Robins, K. A., & Kirtman, B. 2000, J. Phys. Chem. A, 104, 4755
Coonan, M. H., & Ritchie, G. L. D. 1993, Chem. Phys. Lett., 202, 237
Curtiss, L. A., Raghavachari, K., Redfern, P. C., & Pople, J. A. 1997, J. Chem. Phys., 106, 1063
de Boisanger, C., Helmich, E. P., & van Dishoeck, E. F. 1996, A&A, 310, 315
Doty, S. D., & Leung, C. M. 1998, ApJ, 502, 898
Dunbar, R. C. 1994, in Current Topics in Ion Chemistry and Physics, Vol. 2, ed. C. Y. Ng, T. Baer, & I. Powis (New York: Wiley), 279
———. 1997, Int. J. Mass Spectrom. Ion Processes, 160, 1
Dunning, T. H. J. 1989, J. Chem. Phys., 90, 1007
Frisch M. F., et al. 1998, GAUSSIAN 98, Revision A.6 (Pittsburgh: Gaussian, Inc.)
Fukasaku, S., Hirahara, Y., Masuda, A., Kawaguchi, K., Ishikawa, S., Kaifu, N., & Irvine, W. M. 1994, ApJ, 437, 410
Gapeev, A., Yang, C.-N., Klippenstein, S. J., & Dunbar, R. C. 2000, J. Phys. Chem. A, 104, 3246
Graedel, T. E., Langer, W. D., & Frerking, M. A. 1982, ApJS, 48, 321
Guélin, M., Forestini, M., Valiron, P., Ziurys, L. M., Anderson, M. A., Cernicharo, J., & Kahane, C. 1995, A&A, 297, 183
Guélin, M., Lucas, R., & Cernicharo, J. 1993, A&A, 280, L19
Guélin, M., Lucas, R., & Nevi, R. 1997, in IAU Symp. 170, CO: Twenty-Five Years of Millimeter Wave Spectroscopy, ed. W. B. Latter, S. J. E. Radford, P. R. Jewell, J. G. Mangum & J. Bally (Dordrecht: Kluwer), 359
Guélin, M., Muller, S., Cernicharo, J., Apponi, A. J., McCarthy, M. C., Gottlieb, C. A., & Thaddeus, P. 2000, A&A, 363, L9
Guélin, M., Neininger, N., Lucas, R., & Cernicharo, J. 1999, in The Physics and Chemistry of the Interstellar Medium, ed. V. Ossenkopf (Herdecke: GCA), 326
Halkier, A., & Coriani, S. 1999, Chem. Phys. Lett., 303, 408
Herbst, E., & Leung, C. M. 1986, MNRAS, 222, 689
Highberger, J. L., Savage, C., & Ziurys, L. M. 2000, AAS Meeting, 196, 05.11
Hirschfelder, J. O., Curtiss, C. F., & Bird, R. B. 1964, Molecular Theory of Gases and Liquids (New York: Wiley)
Huggins, P. J. 1995, Ap&SS, 224, 281
Kawaguchi, K., Kagi, E., Hirano, T., Takano, S., & Saito, S. 1993, ApJ, 406, L39
Kawaguchi, K., Kasai, Y., Ishikawa, S., & Kaifu, N. 1995, PASJ, 47, 853
Kieninger, M., Irving, K. R., Rivas-Silva, F., Palma, A., & Ventura, O. N. 1998, J. Molec. Struct. (Theochem), 422, 123
Klippenstein, S. J., Yang, Y.-C., Ryzhov, V., & Dunbar, R. C. 1996, J. Chem. Phys., 104, 4502
Kumar, A., & Meath, M. W. 1992, Mol. Phys., 75, 311
Kwan, J. Y., & Linke, R. A. 1982, ApJ, 254, 587
Langer, W. D., et al. 1997, ApJ, 480, L63
Largo-Cabrerizo, A. 1988, Chem. Phys. Lett., 147, 95
Lee, H.-H., Bettens, R. P. A., & Herbst, E. 1996, A&AS, 119, 111
Lucas, R., & Guelin, M. 1998, in IAU Symp. 191, Asymptotic Giant Branch Stars, ed. T. Le Bertre, A. Lebre, & C. Waelkens (San Francisco: ASP), 305
Maroulis, G., & Pouchan, C. 1998, Phys. Rev. A, 57, 2440
Millar, T. J. 1982, in Galactic and Extragalactic Infrared Spectroscopy, ed. P. P. M. F. Kessler & T. D. Guyenne (ESA SP-192; Paris: ESA), 33
Millar, T. J., Farquhar, P. R. A., & Willacy, K. 1997, A&AS, 121, 139
Millar, T. J., & Herbst, E. 1994, A&A, 288, 561
Millar, T. J., Herbst, E., & Bettens, R. P. A. 2000, MNRAS, 316, 195
Millar, T. J., Rawlings, J. M. C., Bennett, A., Brown, P. D., & Charnley, S. B. 1991, A&AS, 87, 585
Ohishi, M., & Kaifu, N. 1998, Faraday Discuss., 109, 205
Oppenheimer, M., & Dalgarno, A. 1974, ApJ, 187, 231
Petrie, S. 1996, MNRAS, 282, 807
———. 1999, MNRAS, 302, 482
———. 2001, J. Phys. Chem. A, 105, 9931
Petrie, S., Becker, H., Baranov, V., & Bohme, D. K. 1997, ApJ, 476, 191
Petrie, S., & Dunbar, R. C. 2000, J. Phys. Chem. A, 104, 4480
Russell, A. J., & Spackman, M. A. 1996, Mol. Phys., 88, 1109
Ryzhov, V., & Dunbar, R. C. 1997, Int. J. Mass Spectrom. Ion Processes, 167/168, 627
Ryzhov, V., Klippenstein, S. J., & Dunbar, R. C. 1996, J. Am. Chem. Soc., 118, 5462
Ryzhov, V., Yang, Y.-C., Klippenstein, S. J., & Dunbar, R. C. 1998, J. Phys. Chem. A, 102, 8865

Scott, A. P., & Radom, L. 1996, J. Chem. Phys., 100, 16502
Soldán, P., Lee, E. P. F., & Wright, T. G. 1998, Trans. Faraday Soc., 94, 3307
Spackman, M. A. 1989, J. Phys. Chem., 93, 7394
Su, T., & Chesnavich, W. J. 1982, J. Chem. Phys., 76, 5183
Truhlar, D. G., Garrett, B. C., & Klippenstein, S. J. 1996, J. Phys. Chem., 100, 12771
Truong-Bach, Graham, D., & Nguyen-Q-Rieu. 1993, A&A, 277, 133
———. 1996, A&A, 312, 565
Turner, B. E., Steimle, T. C., & Meerts, L. 1994, ApJ, 426, L97
Watson, J. N. 1995, Ph.D. thesis, Univ. New England, Armidale
Widmark, P.-O., Persson, B. J., & Roos, B. 1991, Theor. Chim. Acta, 79, 419
Woon, D. E., & Dunning, T. H. J. 1993, J. Chem. Phys., 98, 1358
Ziurys, L. M., Apponi, A. J., & Phillips, T. G. 1994, ApJ, 433, 729
Ziurys, L. C., Savage, C., Highberger, J. L., Apponi, A. J., Guelin, M., & Cernicharo, J. 2001, AAS Meeting, 198, 14.07